

Additional curvature-induced Raman splitting in carbon nanotube ring structures

Yan Ren,^{1,2} Li Song,^{1,2} Wenjun Ma,^{1,2} Yuanchun Zhao,^{3,2} Lianfeng Sun,³ Changzhi Gu,¹ Weiya Zhou,¹ and Sishen Xie^{1,*}
¹Beijing National Laboratory of Condensed Matter Physics, Institute of Physics, Chinese Academy of Sciences, Beijing 100190, People's Republic of China

²Graduate School of Chinese Academy of Sciences, Chinese Academy of Sciences, Beijing 100039, People's Republic of China

³National Center for Nanoscience and Nanotechnology, Chinese Academy of Sciences, Beijing 100190, People's Republic of China

(Received 16 August 2009; published 29 September 2009)

In this paper, a diameter-dependent Raman G band splitting phenomenon in carbon nanotube ring structures is reported and analyzed. In Raman spectra of such structures, more modes became visible as the diameters of rings decrease, and the frequencies of these modes keep unchanged. We attribute this to the resonance condition changes caused by additional curvatures in rings. In this case, perpendicular polarized light would take more effect in rings than in straight tubes as the additional curvature increases, thus intensity enhancements for $E_1(E_{1g})$ and $E_2(E_{2g})$ modes are observed.

DOI: 10.1103/PhysRevB.80.113412

PACS number(s): 78.67.Ch, 61.48.De, 63.22.Gh, 81.07.De

Carbon nanotubes (CNTs) under strain is a topic of wide interest in recent years. Raman frequency shifts and intensity changes in CNTs under strain have been experimentally observed.^{1–6} Most papers in this field mainly focus on strain-induced Raman frequency shifts, however, the details of band structures changes and how it will effect the Raman spectrum have not been well illustrated yet.

The key point in this topic is the magnitude of deformation of tubes under strain. So far the strain can be introduced into tubes in two ways. One is to pull a large bundle of tubes; the other is to manipulate an individual tube by the tip of atomic force microscope (AFM). However, it is difficult to determine the value of strain accurately when these two ways are adopted. On the other hand, ring structures of CNTs have been fabricated in many ways.^{7–10} The diameter of a ring can be measured in scanning electron microscope (SEM) conveniently, which provides an effective way to describe the extent of deformation. Therefore, rings are ideal candidates to analyze the dependence between deformation and spectrum changes quantitatively.

The splitting feature in Raman G band of rings was discovered in our previous work.⁹ In this paper, the splitting is further investigated on individual-ring level and it is found to be diameter dependent. We attributed it to the variation in resonance condition resulted by additional curvatures in rings.

The ring structures of CNTs we used in this experiment were synthesized through floating chemical-vapor deposition method¹¹ similar with the method we adopted to produce rings in large scale.⁹ As mentioned in our previous paper,⁹ the density of rings deposited on substrates can be controlled by growth time and deposit position. In order to get proper density of rings for individual-ring level Raman spectroscopy, the grow time should be restricted within 5 min. Meanwhile, the sublimation process of catalyst precursor was controlled to be sufficiently slow. Figures 1(a) and 1(b) show an orbicular ring and the carbon tube bundles in a ring. The diameters of the rings would vary in the range of 100–400 nm and the majority of them are around 180 nm when ethanol was used as carbon source.

In order to locate the isolated rings in microscope, we deposited them on special substrates [see Fig. 1(c)]. The gold

grids pattern on the substrates was prepared by lithophotography with Karl Suss MA-6 Mask Aligner. These grids serve as the coordinates to locate the isolated rings in this experiment. After being deposited on gridded substrates, the rings were observed in SEM (Hitachi S-5200). The relative positions between isolated rings and the 2.5 μm gold spots (the basic element of the grids) were recorded in a picture with SEM [see Fig. 1(d)]. During this process, areas with low ring densities were chosen to match the micro-Raman resolution ($\sim 1 \mu\text{m}$) to ensure that there was only one ring in the area of laser spot. The labeled spots were located again when the substrate was transferred into micro-Raman microscope (Reinshaw inVia Raman microscope), then the location of the ring could be refound optically with the help of the picture recorded in SEM (the ring is not optically visible for its small size). Finally the spectra of the isolated rings were collected with 514 nm Ar iron laser.

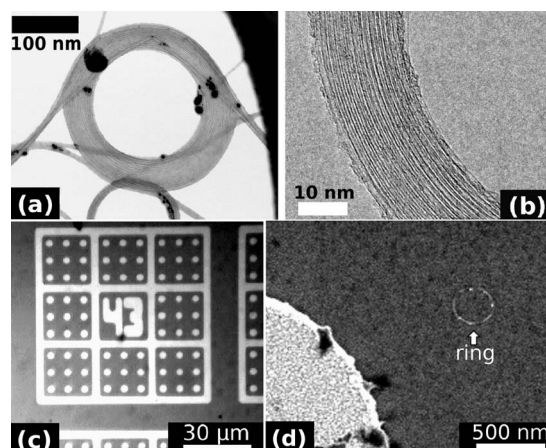


FIG. 1. (a) An orbicular ring (scanning transmission electron microscopy mode, Hitachi S-5200, 30 kV); (b) carbon nanotube bundles in a ring (high-resolution transmission electron microscopy, JEOL 2010, 200 kV); (c) optical image of the grids on silicon substrate. The smallest gold spots in Fig. 1(c) are 2.5 μm in size. They can be located in micro-Raman microscope; (d) SEM image of an isolated ring near a gold spot. The ring is indicated by a white arrow.

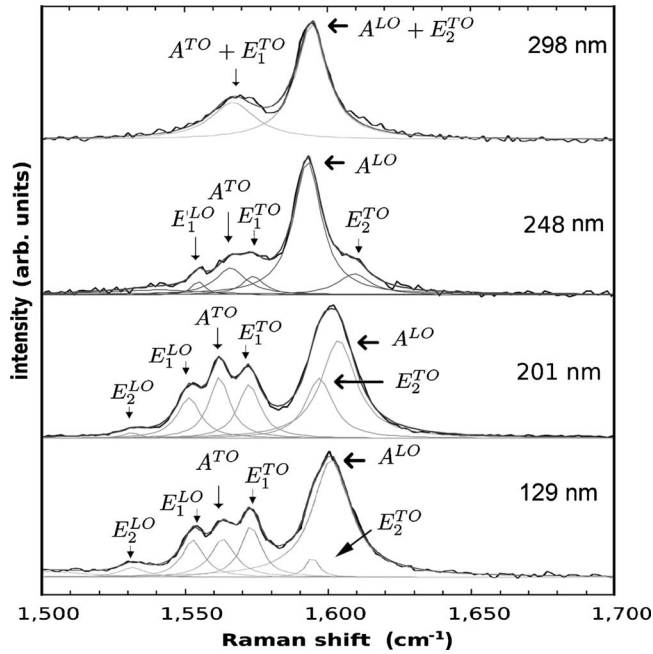


FIG. 2. Raman spectra of rings with different diameters. G band of rings with diameters smaller than 200 nm split into many peaks while the spectra of rings with large diameters are similar with straight tubes. The peaks are assigned to vibrational modes, as denoted in the figure.

Usually Raman G band of CNTs consists of two main components: G^+ and G^- . The G^+ peak around 1592 cm^{-1} dominate the high-frequency region and the G^- peak around 1567 cm^{-1} is weaker than G^+ . Comparing with individual straight tubes¹² or bundles of tubes,¹³ the Raman spectra of rings show new features. Among the spectra of rings we collected, we found that, when the diameters of the rings decreases, the intensities of G^- band increase, meanwhile the whole G band begin to split into more resolvable peaks. Figure 2 shows several typical Raman spectrum for rings with

different diameters. In order to analyze the diameter dependence of the splitting in detail, we normalized all spectra and fitted them with Lorentz line shape to find out the center frequencies and relative intensities of the Raman peaks. During the deconvolution of Raman peaks, we try to find out all the six modes in each spectrum, however, this attempt fails in some spectra due to too weak intensity of certain modes.

Table I gives a list of center frequencies from rings with different diameters, from which we can find another interesting phenomenon: the center frequencies of these peaks don't depend on the diameters of rings but trend to appear around several fixed frequencies [see Fig. 3(b)]. These frequencies can be classified into six groups: $G_1 \sim 1535\text{ cm}^{-1}$, $G_2 \sim 1553\text{ cm}^{-1}$, $G_3 \sim 1563\text{ cm}^{-1}$, $G_4 \sim 1575\text{ cm}^{-1}$, $G_5 \sim 1593\text{ cm}^{-1}$, and $G_6 \sim 1603\text{ cm}^{-1}$, as denoted in Fig. 3(b) and Table I. In many reports about strained tubes, G band frequencies would shift with the strain applied on tubes.¹⁻⁵ As for rings, the Raman peaks show no sign of downshift or upshift but great diversity in frequencies [see Fig. 3(a)]. The strain caused by additional curvature in rings can be calculated by $\delta = d/D$, where δ is the strain, d is the diameter of the tube that constitute the ring, and D is the diameter of the ring. For the rings we measured, δ is in the range of $\pm(0.3-1.3\%)$ (“+” and “-” stand for stretch and compression, respectively), which is not big enough for obvious frequency shifts. This is in accord with the result reported by Lee *et al.*⁶

There are also many reports on the diameter dependence of G band frequencies for straight tubes in which the frequency shifts are attributed to phonon-dispersion induced by circumferential quantum confinement of the tubes.^{12,14-16} However, in our case, there are no clear dependence between the frequencies of the peaks and the diameters of the tubes in the rings. The numbers of resolvable peaks show no dependence on tube diameter as well [see Fig. 3(c)]. Considering the fact that the diameters of the tubes in the rings are in a narrow range (1.2–1.7 nm, evaluating from the frequencies of radial breathing mode), the frequencies variations caused

TABLE I. The resolvable peaks of rings with different diameters. The unit of diameters: nm, Raman frequencies: cm^{-1} . The data in parenthesis gives the relative intensity of the corresponding peak and the most intense peak is taken as a reference.

Diameter	G_1	G_2	G_3	G_4	G_5	G_6
129	1531(0.09)	1552(0.32)	1563(0.32)	1573(0.44)	1594(0.17)	1601(1.00)
139	1537(0.15)	1554(0.48)	1561(0.13)	1578(0.50)	1593(0.13)	1609(1.00)
149	1537(0.15)	1554(0.46)	1562(0.35)	1576(0.46)	1593(0.44)	1607(1.00)
168	1535(0.10)	1552(0.26)	1563(0.35)	1573(0.38)	1592(0.37)	1601(1.00)
178	1537(0.13)	1553(0.42)	1563(0.25)	1572(0.55)	1594(0.48)	1602(1.00)
186	1540(0.06)	1555(0.35)	1564(0.32)	1576(0.42)	1597(1.00)	1608(0.55)
194			1561(0.74)	1577(0.25)	1593(1.00)	1604(0.81)
201	1531(0.05)	1551(0.41)	1562(0.62)	1572(0.55)	1596(0.61)	1603(1.00)
238			1565(0.27)		1590(1.00)	
248	1540(0.03)	1554(0.10)	1565(0.20)	1573(0.14)	1592(1.00)	1609(0.16)
258		1550(0.11)	1559(0.29)	1570(0.34)	1595(1.00)	1603(0.56)
298		1557(0.10)	1567(0.24)	1573(0.15)	1594(1.00)	1609(0.08)
372		1555(0.17)	1565(0.34)	1572(0.20)	1594(1.00)	1601(0.17)

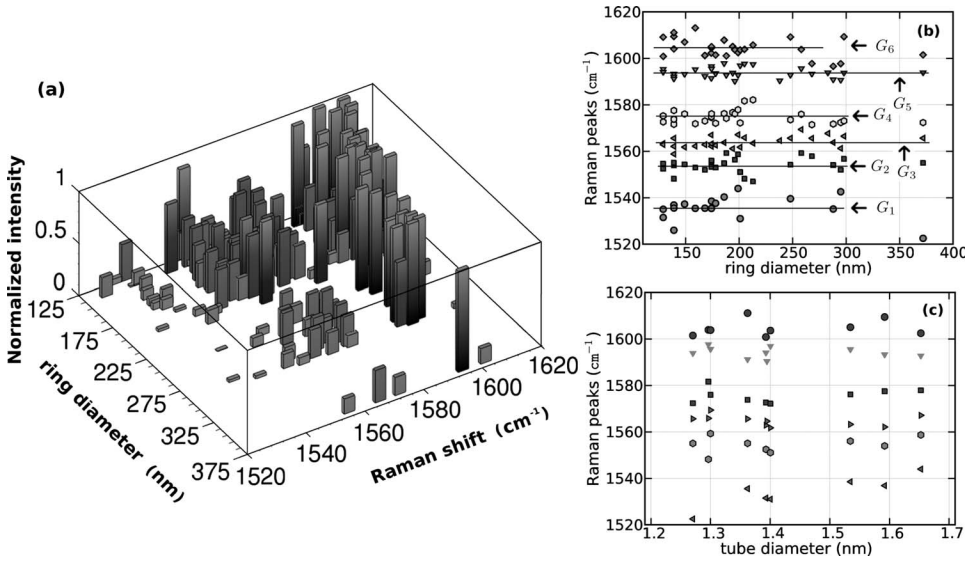


FIG. 3. (a) Three-dimensional bar plot of the frequencies of resolvable Raman peaks, in which the most intense peak is taken as a reference for each diameter; (b) the dependence between frequencies of Raman peaks and ring diameters. The frequencies are classified into six groups. (c) Plot of *G* band peak frequencies vs the diameters of tubes in rings.

by phonon dispersion are of small magnitudes. Theoretical predictions and experimental results have shown that there are six modes [two $A(A_{1g})$, two $E_1(E_{1g})$, and two $E_2(E_{2g})$] in the Raman *G* band of CNTs,^{17,18} however, those six modes have never been observed simultaneously in the previous experiments. In our experiment, up to six resolvable peaks have been found in rings with small diameters. It is natural to assign each peak to a vibrational mode. In straight tubes, the most intense peaks around 1568 and 1590 cm⁻¹ are assigned to unresolvable $A(A_{1g})+E_1(E_{1g})$ and two minor peaks around 1549 and 1602 cm⁻¹ are assigned to $E_2(E_{2g})$ modes based on the polarized Raman results.¹³ But for rings, we cannot distinguish different modes through polarized Raman because of their isotropy in the *XZ* plane. Since totally symmetric modes (*A* modes) are expected to be the most intense peaks in resonance Raman spectra, we assign the most intense peaks at the high-frequency end of *G* band to A^{LO} modes, and peaks around 1563 cm⁻¹ to A^{TO} modes. As the diameter decreases, more resolvable peaks would appear. The newly appeared peaks near A^{LO} modes are assigned to E_2^{TO} modes because E_2^{TO} should have a higher frequency in *G* band.¹⁹ The peaks emerged near A^{TO} modes are assigned to E_1^{LO} and E_1^{TO} modes, these two modes possibly origin from the previously unresolvable $A+E_1$ modes in straight tubes. The peaks with lowest frequencies are assigned to E_2^{LO} modes since E_2^{LO} and E_2^{TO} are expected to have the largest splitting due to both the zone-folding effect and the curvature effect.¹³ When there are less than six resolvable peaks in spectra, some peaks can be assigned as combinations of those modes, as denoted in Fig. 2. Although there are other possible assignments of those peaks, we can conclude that the newly appeared peaks are from E_1 and E_2 modes.

According to the analysis above, the main feature in the spectra of rings is that, the intensities of Raman peaks are strongly diameter dependent. We can conclude that, it is the additional curvature in the rings that dominates the intensities and numbers of the peaks in Raman spectra and the new resolvable peaks emerged belong to $E_1(E_{1g})$ and $E_2(E_{2g})$ modes. Moreover, the relative intensities of these modes in-

crease with increasing additional curvature and become resolvable under a certain diameter.

The dipole selection rule for optical transitions $E_{\mu'}^v \rightarrow E_{\mu}^c$ between the subbands of nanotubes is $\mu' = \mu$ for light polarized parallel to the tube axis and $\mu' = \mu \pm 1$ for light polarized perpendicular to the axis.^{20–22} It is reported that optical properties of CNTs show strong anisotropy, absorption and scattering are suppressed for light polarized perpendicular to the tube axis, this is called depolarization effect or antenna effect.^{23,24} However, according to the results of polarized resonance Raman of CNTs, the $E_{\mu}^v \rightarrow E_{\mu \pm 1}^c$ transitions needs to be considered to illustrate the experimental results.¹⁶ When the energy gap between the two subbands match the photon energy of incident laser, $E_{\mu}^v \rightarrow E_{\mu \pm 1}^c$ transitions would contribute considerable intensity as well.

We select the nanotube axis in the *Z* direction, let light incident along *Y* direction, and collect the backscattering light. Jorio *et al.*¹⁶ has proposed the selection rules for resonance Raman of CNTs

$$\begin{array}{c}
 \parallel \quad A(ZZ) \quad \parallel \\
 E_{\mu}^v \rightarrow E_{\mu}^c \rightarrow E_{\mu}^c \rightarrow E_{\mu}^v \\
 \parallel \quad E_1(ZX) \quad \perp \\
 E_{\mu}^v \rightarrow E_{\mu}^c \rightarrow E_{\mu \pm 1}^c \rightarrow E_{\mu}^v \\
 \perp \quad A(XX) \quad \perp \\
 E_{\mu}^v \rightarrow E_{\mu \pm 1}^c \rightarrow E_{\mu \pm 1}^c \rightarrow E_{\mu}^v \\
 \perp \quad E_1(XZ) \quad \parallel \\
 E_{\mu}^v \rightarrow E_{\mu \pm 1}^c \rightarrow E_{\mu}^c \rightarrow E_{\mu}^v \\
 \perp \quad E_2(XX) \quad \perp \\
 E_{\mu}^v \rightarrow E_{\mu \pm 1}^c \rightarrow E_{\mu \mp 1}^c \rightarrow E_{\mu}^v
 \end{array}$$

When the incident light is parallelly polarized along *Z*, $E_{\mu}^v \rightarrow E_{\mu}^c$ transitions are allowed. $A(A_{1g})$ can be observed in the (*ZZ*) scattering geometry and $E_1(E_{1g})$ modes can be observed in the (*ZX*) geometry, in this case, $E_2(E_{2g})$ mode donot appear; when the light is perpendicularly polarized, $E_{\mu}^v \rightarrow E_{\mu \pm 1}^c$ transitions occur, in this case $A(A_{1g})$ and $E_2(E_{2g})$ modes can be observed in the (*XX*) geometry, while $E_1(E_{1g})$ would appear in the (*XZ*) geometry.

The Raman intensity is determined by two factors: optical transitions probability and electron-phonon coupling. In

CNTs, optical transition is the dominating factor.²⁵ In our case, the intensities of $E_1(E_{1g})$ and $E_2(E_{2g})$ are enhanced in the spectra of rings, which indicates that $E_{\mu}^v \rightarrow E_{\mu\pm 1}^c$ transitions are playing a more important role in rings than in straight tubes. One possible reason is, the depolarization effect is not so strong as in straight tubes in rings due to their special isotropic shape. On the other hand, as a result of additional curvature, two kinds of strain (both stretch and compression) coexist in a ring, and the magnitude of strain varies from the inner edge to the outer edge. When tubes become strained or bent, there will be bend-induced gap,^{3,26,27} gap energy changes,^{2,27,28} localized gap states,^{29,30} and asymmetric change in electronic structure.³¹ The changes in electronic structures will affect the intensities, profiles, and frequencies of Raman peaks of CNTs.^{1,3,5,6} At the presence of additional curvatures, similar mechanism may occur in rings. The changes in electronic structure would make the $E_{\mu}^v \rightarrow E_{\mu\pm 1}^c$ transitions resonate with the incident laser more efficiently, which consequently enhance the intensities of $E_1(E_{1g})$ and $E_2(E_{2g})$ modes in the Raman spectra.

In summary, we reported and analyzed the diameter-dependent Raman G band splitting in carbon nanotube ring structures. We found that new peaks emerge in G band of ring's Raman spectrum as the ring's additional curvature increases and the intensities of the peaks also show dependence on the additional curvature. However, the frequencies of Raman modes do not change with this curvature. We supposed that, in the presence of additional curvature, the electronic structures and resonance windows of rings would become favored for perpendicular polarized light, thus the intensities of the $E_1(E_{1g})$ and $E_2(E_{2g})$ modes are enhanced, consequently more Raman modes become resolvable in the spectra.

The authors would like to thank P. H. Tan and Y. J. Guo for their help in Raman measurements, C. Y. Wang for SEM, X. A. Yang for TEM, J. J. Li, Z. Liu, and C. Y. Qiu for preparing the substrates. This work is supported by "973" National Key Basic Research Program of China (Grant No. 2005CB623602) and the key item of knowledge innovation project of Chinese Academy of Science under Grant No. KJCX2-YW-M01.

*ssxie@aphy.iphy.ac.cn

- ¹S. B. Cronin, A. K. Swan, M. S. Ünlü, B. B. Goldberg, M. S. Dresselhaus, and M. Tinkham, *Phys. Rev. Lett.* **93**, 167401 (2004).
- ²S. B. Cronin, A. K. Swan, M. S. Ünlü, B. B. Goldberg, M. S. Dresselhaus, and M. Tinkham, *Phys. Rev. B* **72**, 035425 (2005).
- ³A. G. Souza Filho, N. Kobayashi, J. Jiang, A. Gruneis, R. Saito, S. B. Cronin, J. Mendes Filho, G. G. Samsonidze, G. Dresselhaus, and M. S. Dresselhaus, *Phys. Rev. Lett.* **95**, 217403 (2005).
- ⁴R. Kumar and S. B. Cronin, *Phys. Rev. B* **75**, 155421 (2007).
- ⁵X. Duan, H. Son, B. Gao, J. Zhang, T. Wu, G. Samsonidze, M. Dresselhaus, Z. Liu, and J. Kong, *Nano Lett.* **7**, 2116 (2007).
- ⁶S. Lee, G.-H. Jeong, and E. Campbell, *Nano Lett.* **7**, 2590 (2007).
- ⁷R. Martel, H. R. Shea, and P. Avouris, *Nature (London)* **398**, 299 (1999).
- ⁸M. Sano, A. Kamino, J. Okamura, and S. Shinkai, *Science* **293**, 1299 (2001).
- ⁹L. Song, L. J. Ci, L. F. Sun, C. H. Jin, L. F. Liu, W. J. Ma, D. F. Liu, X. W. Zhao, S. D. Luo, Z. X. Zhang, Y. J. Xiang, J. J. Zhou, W. Y. Zhou, Y. Ding, Z. L. Wang, and S. S. Xie, *Adv. Mater. (Weinheim, Ger.)* **18**, 1817 (2006).
- ¹⁰S. Zou, D. Maspoch, Y. Wang, C. Mirkin, and G. Schatz, *Nano Lett.* **7**, 276 (2007).
- ¹¹H. M. Cheng, F. Li, G. Su, H. Y. Pan, L. L. He, X. Sun, and M. S. Dresselhaus, *Appl. Phys. Lett.* **72**, 3282 (1998).
- ¹²A. Jorio, A. G. Souza Filho, G. Dresselhaus, M. S. Dresselhaus, A. K. Swan, M. S. Ünlü, B. B. Goldberg, M. A. Pimenta, J. H. Hafner, C. M. Lieber, and R. Saito, *Phys. Rev. B* **65**, 155412 (2002).
- ¹³A. Jorio, G. Dresselhaus, M. S. Dresselhaus, M. Souza, M. S. S. Dantas, M. A. Pimenta, A. M. Rao, R. Saito, C. Liu, and H. M. Cheng, *Phys. Rev. Lett.* **85**, 2617 (2000).
- ¹⁴A. Kasuya, Y. Sasaki, Y. Saito, K. Tohji, and Y. Nishina, *Phys. Rev. Lett.* **78**, 4434 (1997).
- ¹⁵O. Dubay, G. Kresse, and H. Kuzmany, *Phys. Rev. Lett.* **88**, 235506 (2002).
- ¹⁶A. Jorio, M. A. Pimenta, A. G. Souza Filho, G. G. Samsonidze, A. K. Swan, M. S. Ünlü, B. B. Goldberg, R. Saito, G. Dresselhaus, and M. S. Dresselhaus, *Phys. Rev. Lett.* **90**, 107403 (2003).
- ¹⁷R. Saito, G. Dresselhaus, and M. Dresselhaus, *Physical Properties of Carbon Nanotubes*, 1st ed. (Imperial College, London, 1998).
- ¹⁸M. S. Dresselhaus and P. C. Eklund, *Adv. Phys.* **49**, 705 (2000).
- ¹⁹R. Saito, A. Jorio, J. H. Hafner, C. M. Lieber, M. Hunter, T. McClure, G. Dresselhaus, and M. S. Dresselhaus, *Phys. Rev. B* **64**, 085312 (2001).
- ²⁰M. F. Lin, *Phys. Rev. B* **62**, 13153 (2000).
- ²¹A. Gruneis, R. Saito, G. G. Samsonidze, T. Kimura, M. A. Pimenta, A. Jorio, A. G. Souza Filho, G. Dresselhaus, and M. S. Dresselhaus, *Phys. Rev. B* **67**, 165402 (2003).
- ²²S. V. Goupalov, *Phys. Rev. B* **72**, 195403 (2005).
- ²³H. Ajiki and T. Ando, *Physica B (Amsterdam)* **201**, 349 (1994).
- ²⁴G. S. Duesberg, I. Loa, M. Burghard, K. Syassen, and S. Roth, *Phys. Rev. Lett.* **85**, 5436 (2000).
- ²⁵S. Reich, C. Thomsen, G. S. Duesberg, and S. Roth, *Phys. Rev. B* **63**, 041401(R) (2001).
- ²⁶L. F. Chibotaru, S. A. Bovin, and A. Ceulemans, *Phys. Rev. B* **66**, 161401(R) (2002).
- ²⁷E. D. Minot, Y. Yaish, V. Sazonova, J.-Y. Park, M. Brink, and P. L. McEuen, *Phys. Rev. Lett.* **90**, 156401 (2003).
- ²⁸H. Maki, T. Sato, and K. Ishibashi, *Nano Lett.* **7**, 890 (2007).
- ²⁹A. Rochefort, P. Avouris, F. Lesage, and D. R. Salahub, *Phys. Rev. B* **60**, 13824 (1999).
- ³⁰M. S. C. Mazzoni and H. Chacham, *Phys. Rev. B* **61**, 7312 (2000).
- ³¹B. Shan, G. W. Lakatos, S. Peng, and K. Cho, *Appl. Phys. Lett.* **87**, 173109 (2005).